



Since 1969

journal homepage: [www.piche.org.pk/journal](http://www.piche.org.pk/journal)

## Evaluation of Hydrothermally Carbonized Alternative Biomass (*Lepironia Articulata*) as a Source of Alternative Energy and Adsorbent

Asadullah\*<sup>1,2</sup>, L. Kaewsichan<sup>1</sup>, K. Tohdee<sup>1</sup>

Submitted: 28/05/2019, Accepted: 19/08/2019, Online: 19/08/2019

### Abstract

*Lepironia articulata* (LA) widely available wetland biomass was successfully converted into a solid coal-like material called hydrochar. Hydrothermal carbonization (HTC) being a technically-attractive thermal conversion process of biomass into hydrochar at mild conditions was adopted in this study. The effect of process parameters on the physicochemical properties and the yield of hydrochar was studied by varying carbonization temperature and residence time over the range of 180, 200, 220, 240 °C and 6, 12, 24 h, respectively. With an increase in temperature, the hydrochar yield decreased rapidly from 68.8% at 180 °C to 55.2% at 240 °C. In addition, the increase in carbon percentage was observed with an increase in temperature from 10.28% (180 °C) to 38.69 % (240 °C). The H/C and O/C atomic ratios reduced from 1.392 and 0.541 to 1.072 and 0.271, respectively, which was typically related to decarboxylation, demethanation, and dehydration reactions. Hydrochar obtained was characterized appropriately, i.e., proximate analysis, TGA, HHV, FT-IR and BET. The highest surface area ( $S_{BET}$ ) of hydrochar obtained was 72.2  $m^2/g$ . The maximum iodine number calculated was 220 mg/g. HHV of hydrochar was in the range of 22.52 to 25.1 MJ/kg. Overall results conclude the effectiveness of LA in the field of environmental remediation, sustainable and alternative energy.

**Keywords:** Hydrothermal carbonization, Dehydration, Decarboxylation, Demethanation

### 1. Introduction:

Biomass has been widely used strategically for sustainable consumption. Additionally, to being a renewable raw material and a food source, it can be used for energy production [1], carbon sequestration [2], wastewater treatment and, finally, as a vital constituent to increase soil fertility. To get the maximum yield out of it, biomass is converted into a solid char product, which could be further modified and treated to make it more

useful for mentioned applications. There were several carbonization methods for the production of biochar, including gasification, pyrolysis, flash carbonization and hydrothermal carbonization[3]. Variety of biomass was converted into these valuable products by researchers from time to time, considering the availability, cost of biomass, conversion process, and process environmental drawbacks. HTC is said biomass conversion via thermal carbonization technique yields a liquid and

<sup>1</sup> Department of Chemical Engineering, Faculty of Engineering, Prince of Songkla University, Hat Yai, Songkhla 90112 Thailand.

<sup>2</sup> Department of Chemical Engineering, Faculty of Engineering and Architecture, Balochistan University of Information Technology, Engineering and Management Sciences, Quetta.

\*Corresponding Author: asad1562000@yahoo.com

carbon (C)-rich solid called hydrochar. In soil, this hydrochars may act as fertilizers and promote C sequestration [2]. On the way towards the conversion of biomass into the different solid and liquid product via HTC process, made this an attractive method due to, cost-effectiveness, less energy consumption, high yield, easy handling, and finally environmentally less hazardous due to no open gas ventilation into the air. Reported by Shimin *et al* [4], during HTC process some gases, such as nitrogen oxides,  $\text{CO}_2$  and sulfur oxides, forming the corresponding acids and/or salts after being dissolved in water, so that no further treatment for air pollution is required. Many reporters have concluded this process to be the best amongst all other biomass conversion methods i.e., slow and fast pyrolysis, microwave assisted pyrolysis, gasification and direct heated, etc [5-7]. It was also noticed through different researchers that various products could also be obtained by only applying a small treatment on the hydrochar and liquid products obtained from the HTC process. Ying *et al* [8], obtained variable products and highest yield by using different biomass as rice straw (RS), and water hyacinth (WH), he got highest heavy oil yield from RS of 21.62% and 12.19% from WH under process conditions of liquefaction at 300 °C for 30 min followed by carbonization at 220 °C for 4 h, respectively. Denso-Boateng *et al* [9], obtained hydrochar, liquid, and gas products by treating primary sewage sludge using HTC process at temperatures ranged (140, 160, 180 and 200 °C), respectively, they observed a decrease in carbon contents retained in hydrochars as temperature and time increased with carbon retentions of 647.7% at 140 and 160 °C, and 50.62% at 180 and 200 °C, respectively. The final product yield and its capacity according to its use significantly depend upon the conditions during the HTC process. Kannan S *et al* [10], while treated shrimp waste concluded that the HTC holding time of 112 min and holding temperature of 184 °C produced the highest yield (42%) of hydrochar and the ash content and atomic carbon content of the hydrochar were found to be 21-25%, 39-49%,

respectively. Cai J *et al* [11], converted tobacco stalk into hydrochar using HTC method, He noticed an increase in the carbon contents of hydrochars (46.5-65.2%), while a decrease in hydrogen and oxygen contents (5.2-5.8% and 16.2-42.1%), respectively. The obtained hydrochars possessed lower volatile (42.4-75.7%), higher fixed carbon (15.6-48.8%) and higher HHV (18.7-27.2 MJ kg<sup>-1</sup>). Therefore, optimum process conditions should be applied to get the highest yield and maximum useful properties.

LA or Krajood grass (local name) is widely cultivated in Thale Noi wetland area as well as from other areas such as Nakhon Si Thammarat, Narathiwat southern regions of Thailand. In this study sustainability of biomass (LA), obtained from Thale Noi district was assessed for the first time, after converting it into hydrochar using HTC process. The schematic diagram of HTC products for possible applications is given in Figure 1. Furthermore, hydrochar obtained at different temperatures and residence time were characterized for their potential applications. It is assumed that the chemical composition of the raw material (*lepironia articulata*) determines the properties of the solid HTC products, including the study of factors that could affect their degradability. Therefore, LA obtained was characterized first and the characterization of hydrochar products was continued to be done after applying variable process conditions, by varying temperature, water to biomass ratio (WTB), and retention time, respectively.

## 2. Materials and methodology:

### 2.1 Materials:

The main ingredient of this study was the biomass (LA) obtained from the coastal belt of Thale Noi, Paththalung district, Thailand. All other chemicals and reagents were obtained from Sigma Aldrich chemicals (Thailand).

### 2.2 Methodology:

#### 2.2.1 Production of hydrochar:

The feedstock (LA) after reduced to the desired particle size was added to a 1 L Teflon lined

stainless reactor (Figure 1). The reactor was equipped with a thermocouple and a pressure gauge to monitor inside temperature and pressure of the reactor. The inside temperature was varied by insulating an electric heating jacket covered with a robust outer safety shell. PID controller was used to maintaining the temperature of the mixture inside to 180 °C, 200 °C, and 220 °C and 240 °C for the residence time 2, 4, and 6 h, respectively. The LA to deionized (DI) water ration was kept constant (1:10) throughout the experiments due to the reason that in previous studies it was confirmed to the best value to get optimum characteristics of hydrochar

[7, 11, 12]. After completion of the process cycle, the reactor was allowed to cool to room temperature. The resultant hydrochars were then isolated by filtration using 0.45 mm dia (Whatman) filter paper, washed by rinsing warm DI water various times to remove water-soluble volatile matter, and dried by keeping in the oven for 4 h at 105 °C. The hydrochar samples obtained were labeled based on their production properties (time and processing temperature). The detailed process schematic can be seen at Figure 2.

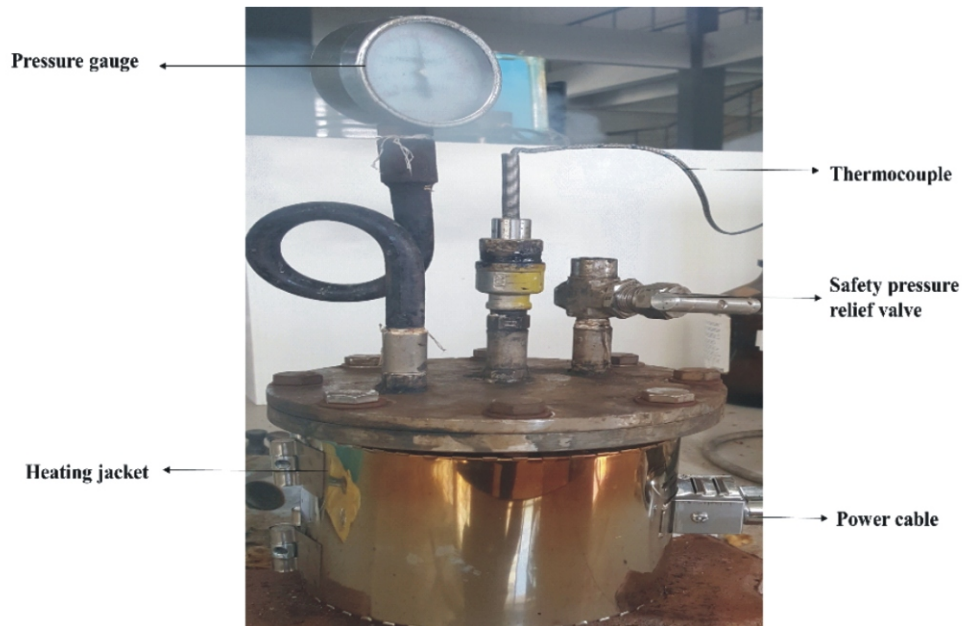


**Figure 1.** Hydrothermal reactor

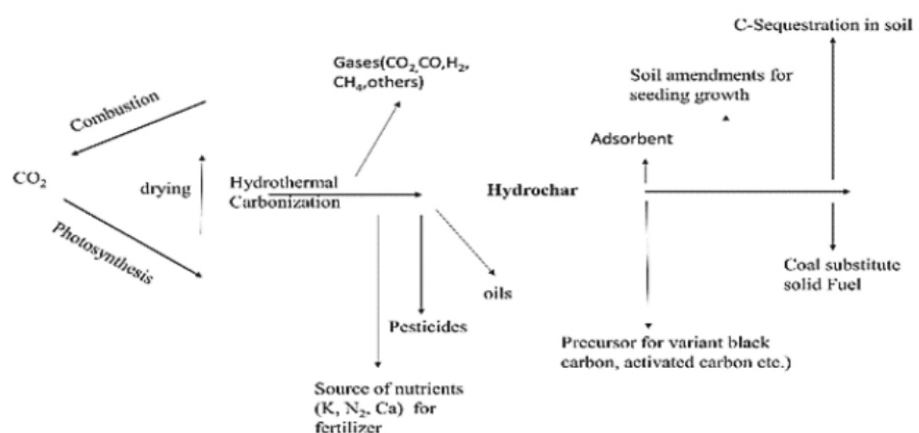


**Figure 2:** Schematic of HTC process with possible products and their applications

% Yield of the product hydrochars was determined by dividing the weight of dry Hydrochar to the weight of dry raw biomass (LA) as shown in eq.(1).

$$\text{Hydrochar yield}(\%) = \frac{\text{mass of recovered solid after HTC(dry basis)}}{\text{initial mass of biomass LA(dry basis)}} \times 100 \quad (1)$$

### 2.2.2 Characterization:

A CHN organic Elemental Analyzer (Macro FLASH 2000) was used to determine the carbon, Nitrogen, and hydrogen contents of hydrochars. The contents of Oxygen was calculated from the outstanding mass fraction by excluding the ash content. The volatile matter (VM) and ash contents including proximate analysis were analyzed by the standard method of ASTM D 7582 [13] and NREL/TP-510-42622 [14], respectively. The remaining fixed carbon (FC) was calculated by subtracting the ash content and VM from the total mass. A thermogravimetric analyzer (TGA7, Perkin Elmer, USA) was used to analyze the thermal decomposition behaviors of hydrochar in the temperature range of 50 - 1000 °C at 10 °C/min of heating rate with 20 mL N<sub>2</sub>/min. The chemical functional groups developed on the surface of hydrochar were distinguished by FTIR spectroscopy. Infrared spectra (4000 - 400 cm<sup>-1</sup>) were attained based on the diamond attenuated total reflectance (ATR) method using an FT-IR Spectrometer (Bruker Vortex 70 spectrometer, Germany) at a resolution of 4 cm<sup>-1</sup> by using 64 scans. Surface area, pore volume, and porosity of the hydrochar samples were analyzed using BET, ASAP2460, Micromeritics, USA. An updated van-Soest method using Pyrex® (Gooch) crucible was used to determine the contents of cellulose, hemicellulose, aqueous soluble compounds, and pseudo-lignin in the raw biomass (LA) and solid LAHC samples[15]. The LA and LAHC samples are converted into the desired particle size (20-65 mesh) after crushing and sieving. Prior to the analysis, samples were dried at 105 °C for 24 h to remove any unnecessary moisture content if present. The contents of cellulose, lignin, and hemicellulose, were calculated from the difference of acid detergent fiber (ADF), neutral detergent fiber

(NDF), acid detergent lignin (ADL), and ash from the following equations [16];

$$\text{Extractive} (\%) = 100 - \text{NDF}(\%) \quad (2)$$

$$\text{Hemicellulose} (\%) = \text{NDF}(\%) - \text{ADF}(\%) \quad (3)$$

$$\text{Cellulose}(\%) = \text{ADF}(\%) - \text{ADL}(\%) \quad (4)$$

$$\text{Pseudo-lignin}(\%) = \text{ADL}(\%) - \text{Ash}(\%) \quad (5)$$

Higher heating value (HHV) was estimated according to the formula of Channiwala and Parikh (2002)[17].

$$\text{HHV}(\text{MJ/Kg}) = 0.3491\text{C} + 1.1783\text{H} + 0.1005\text{S} - 0.10340 - 0.015\text{N} - 0.021\text{A} \quad (6)$$

Where, C, S, H, N, O and A symbolize carbon, sulfur, hydrogen, nitrogen, oxygen, and ash content (wt.% dry basis), respectively.

## 3. Results and Discussion:

### 3.1 Hydrochar yield:

The effect of reaction parameters on hydrochar yield is listed in Table 1. It can be seen that deviations in hydrochar yield are largely depended on the HTC process reaction temperature. The hydrochar yield decreased in the range (68.8 - 56.72) from 180 °C to 220 °C, respectively. The significant decrease in hydrochar yield due to increasing the production temperature was likely because, at higher HTC temperatures, a larger degree of biomass decomposition occurred; hence, more volatilization of biomass tends to decrease biochar yield [18]. Another reason could be the lower lignin and highest cellulose and hemicellulose components present in LA, which was previously concluded in a study, where, Kang *et al* (2012)[19], obtained the maximum hydrochar yield during HTC compared to pinewood meal and pure cellulose. The reason is that the strong phenolic structure of lignin doesn't allow it to synthesize into liquid and gaseous fractions at low HTC temperatures [20]. The effect of holding time on

hydrochar yield was assessed in the range of (2, 4, and 6 h) at different temperatures and constant BTW ratio 1:10. On average a decrease of 2-3.5 % of yield was observed for 2-6 h holding time for all the temperatures. The reason for the low effect of holding time on hydrochar yield is due to the stable reaction conditions and the biomass structures

were being degraded to reduced, dissolvable products. Generally, it was identified that high water content makes the reaction more severe, whereas, low water content can decrease the degradation rate and also cause a decrease in hydrochar yield.

**Table 1:** Lignocellulosic component and hydrochar yield by varying reaction parameters

Sample	Reaction Conditions		Hydrochar yield( wt % dry raw material)	Ash (wt% dry hydrochar)	Hemicellulose (wt% dry hydrochar)	Cellulose (wt% dry hydrochar)	Lignin (wt% dry hydrochar)
	Temperature (°C)	Time (h)					
Raw LA	--	--	--	14.3	30	36.7	19
LAHC-180-2	180	2	68.8	12.7	27.6	27.7	42.9
LAHC-180-4		4	67.6	12.05	26.54	27.22	42
LAHC-180-6		6	66.45	12.46	26	26.45	40.88
LAHC-200-2	200	2	64.85	12.7	13.4	12.4	52.24
LAHC-200-4		4	64	12	13.11	11.87	51.22
LAHC-200-6		6	63.12	11.89	13	11.69	51
LAHC-220-2	220	2	61.35	10.6	12.6	12.8	57.3
LAHC-220-4		4	60.56	10.22	12.65	12.08	57.22
LAHC-220-6		6	58.23	11.05	12.22	12.11	56.89
LAHC-240-2	240	2	56.725	8.87	9.84	10.24	61.55
LAHC-240-4		4	56	8.54	8.96	9.25	60.21
LAHC-240-6		6	55.2	7.21	8.25	9.11	59.65

### 3.2 Lignocellulosic Composition of Hydrohars:

Table 1 illustrates the lignocellulosic fraction of hydrochar obtained from HTC against the different reaction times and temperatures. The lignocellulosic fraction of raw LA was composed of 30, 36.7, 19, of hemicellulose, cellulose, and lignin, respectively. By increasing the reaction temperature from 180 to 240 °C significantly decreased cellulose and hemicellulose contents and where the highest degradation of 80% and 67% were observed at 240 °C for hemicellulose and cellulose,

respectively. Meantime, Lignin content increased continuously and the maximum increase of 70% was observed at 240 °C. The degradation products of hemicellulose via polymerization and condensation reaction was the baseline for the formation of more hydrochar (pseudo-lignin) which consequently was the reason for an increase in lignin content [21]. Simply, as the rate of polymerization and condensation were dominating that of decomposition, that result in optimum hydrochar yield, e.g. the condition between 180 °C and 200 °C. At low temperature between (180 °C and 200 °C), it

was likely that hydrolysis was the predominating reaction [15, 18], and as a result, hemicellulose decreased rapidly and converted into liquid products. The rate of reaction severity increased by limiting the water quantity in the system and raising the temperature, which led the hemicellulose to decrease further at BTW of 1:10. The reduction in hemicellulose decomposition was lower with an increase in holding time as compared to the increase in temperature. The same trend was observed with cellulose and lignin. Overall to hydrolyze cellulose was found more difficult than hemicellulose due to its different behavior during the HTC process [23].

### 3.3 Proximate and Ultimate Analysis For Energy Potential:

The effects of reaction temperature on compositions from ultimate and proximate analyses are summarized in Table 2. Based on previous characterization results and keeping in view that there was not a considerable impact of reaction holding time on product characteristics, the optimum holding time of 2 h was chosen for further analysis. Increasing reaction temperature from 180 to 240 °C improved the carbon content, whilst decreased hydrogen and oxygen contents. This was attributed to the decarboxylation and dehydration reactions taken place during HTC [24], and this is corresponding to a decrease of hydrogen to carbon (H/C) ratio, and oxygen to carbon (O/C) ratio. Proximate analyses of the raw and treated samples demonstrated that increasing the reaction temperature from 180 to 240 °C have increased the fixed carbon (FC) and reduced the volatile matter (VM) and ash contents. Similar kind of observations was found through HTC experiments on food waste, grape marc [20, 21]. This trend was predictable due to at a high temperature of some inorganics components were re-precipitation onto the hydrochar, as was also proposed earlier by [26]. A further calculation towards the energy potential of the product revealed that an increase in the reaction temperature from 180 to 240 °C enhanced the HHV of LAHC samples from 22.25 to 24.95 MJ/kg. Both of the values are higher than the HHV

of raw biomass LA being 18.955. Above illustrations were further explained via Van-Krevelen diagram (Fig.2). Van Krevelen diagrams basically allow for delineation of reaction pathways and propose a clear insight into the chemical transformations of the carbon-rich material, which are, dehydration, demethanation, and de-carboxylation (the depletion of carboxylic groups in the form of CO<sub>2</sub>) [7]. Figure 3 shows a decrease in both the H/C and O/C atomic ratios with an increase in reaction temperature. The dehydration path at high-temperature operation is predominant as compared to the lower temperature operation. It is proposed that during the hydrothermal process, decarboxylation occurs as a side reaction because at complete dehydration reaction water molecules get eliminated from the samples [24, 25]. The hydrochar synthesized at 240 °C for 2 h and BTW of 1:10 has the highest HHV of 24.95 MJ/kg dry, which is relative with the low-rank coal substitute material (lignite), and subsequently, these process conditions were recognized for the manufacture of hydrochar as an alternate energy source. The HHV value obtained from current study was found better when compared with the HHV Value of 21 MJ/kg obtained from similar kind of biomass in a previous research [29]. In conclusion, HTC of LA at raised up temperature to 240 °C, or at optimum moisture content could generally lead to the improved heating value of the hydrochar product.

To better understand the energy outcome of different hydrochar products, Energy yields were calculated based on their HHVs and applying the following Eq.(3 & 4)

$$EY(\%) = HY \times ED \quad (7)$$

$$ED = \frac{HHV \text{ of dried hydrochar}}{HHV \text{ of dried biomass(LA)}} \quad (8)$$

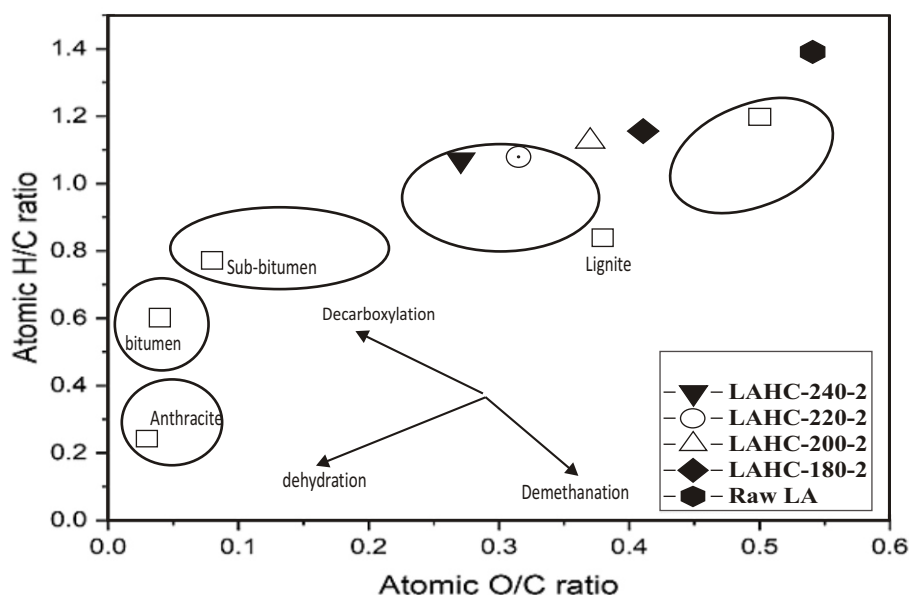
Where EY= energy yield in (%); HY= hydrochar yield (%); ED=energy densification

**Table 2:** Proximate analysis, ultimate analysis, and higher heating value of LA and its derived hydrochar

		LA	LAHC-180-2	LAHC-200-2	LAHC-220-2	LAHC-240-2
Proximate analysis(wt.%,db)	Ash	14.7	12.7	10.6	8.8	7.24
	VM	64.9	61.5	57.07	55.27	51.21
	FC	20.4	25.8	32.33	35.93	41.55
	FC/VM	0.31	0.42	0.56	0.65	0.81
Fuel ratio	C	46.58	55.2	58.67	60.25	62.64
	H	5.44	5.36	5.21	4.96	4.68
	N	1.37	1.38	1.3	1.29	1.27
	S	0.86	0.86	0.86	0.86	0.86
Ultimate analysis(wt.%,db)	O	33.59	30.25	28.88	25.32	22.65
	H/C	1.39	1.15	1.05	0.98	0.89
	O/C	0.54	0.41	0.37	0.31	0.27
	HHV(MJ/kg)		18.95	22.25	23.47	24.14
HHV <sub>daf</sub> (MJ/kg)		19.26	22.52	23.70	24.32	25.10

db = dry basis

daf = dry ash-free

**Figure 3:** Van Krevelen diagram of hydrochars from HTC process indicating the location of raw LA, hydrochars from different reaction temperatures and times

### 3.4 Surface Area and Porosity:

Surface area, pore size and pore volume of hydrochar samples obtained at optimized conditions were analyzed. Table 3 illustrates the data related to the BET surface area of LAHCs and their comparison with previous reference data. The obtained results were verified by repeating the tests and by taking the mean of the two measurements to signify each assessment. These results indicate that BET surface area, total pore volume, and average pore diameter of hydrochar products increased by increasing the HTC temperature from 180 to 220 °C up to  $72.2 \text{ m}^2/\text{g}$ , afterward further increase in temperature to 240 °C tends to decrease the surface area and pore volume to  $70.25 \text{ m}^2/\text{g}$  and  $0.076 \text{ cm}^3/\text{g}$ , respectively. The reason for the decrease in surface area of LAHC products is due mainly to the pore

wall collapse as a result of deformation, fusion, and melting at high HTC temperature [20]. When comparing with dry pyrolysis chars it happens at a lower temperature threshold for hydrochars, possibly because during HTC experiments the pressure increases with the increase in temperature[30]. In the beginning, with an increase in HTC temperature to 220 °C BET surface area increased due to the widening of the pore structure of hydrochars [31]. These results reveal that hydrochar properties are strongly dependent on the process parameters of HTC such as reaction time and temperature. Furthermore, it is suggested that for high adsorption applications the surface area and porosity of hydrochars could be upgraded by thermal and chemical activation methods.

**Table 3.** Comparison of surface area, pore size, pore volume, energy yield, and adsorbent capacity of different hydrochar materials

Sample	Adsorbate	HTC parameters	Surface Area (m <sup>2</sup> /g)	Pore Volume (cm <sup>3</sup> /g)	Pore size Å	q <sub>e</sub> (mg/g)	Energy Yield	Reference
LAHC-180-2	Iodine	Temp =180 °C, time=2hr	67.86	0.079	47	174	80.44	This study
LAHC-200-2	Iodine	Temp =200 °C, time=2hr	69.23	0.080	46.23	196	81.14	This study
LAHC-220-2	Iodine	Temp =220 °C, time=2hr	72.20	0.901	53.6	216	79.35	This study
LAHC-240-2	Iodine	Temp =240 °C, time=2hr	70.25	0.076	43.65	220	77.24	This study
Tobacco stalk	NA	Temp=260 C, time=4hr	11.27	0.057	14.866	NA	63.56	[11]
Coal fly ash	Iodine	mechanical activation	69.00	0.180	63	238	NA	[32]
Rice husk	zinc	Temp=300, time=6hr	20.30	0.074	NA	0.001	NA	[7]
Macadamia shells	NA	Temp=260	12.60	0.036	113	NA	NA	[33]
Plant biomass	lead, Phosphate	Temp=200	10.70	0.215	NA	NA	NA	[20]

### 3.5 FTIR Spectra:

Functional groups play a vital role during the adsorption of contaminants from wastewater. It also identifies some important compounds which support the energy potential of the biomass or char material. Therefore for comprehensive analysis, FTIR spectrum of raw biomass LA and LAHC-180-2, LAHC-200-2 and LAHC-220-2 were analyzed at the range of  $400 \text{ cm}^{-1}$  to  $4000 \text{ cm}^{-1}$ . The HTC char produced in these experiments shows three major absorption bands in the functional group region of the IR spectrum. The region in between  $3200 \text{ cm}^{-1}$  -  $3600 \text{ cm}^{-1}$  shows a broad band which indicates the presence of OH functional group. This band is more usual at lower reaction temperatures since more of an oxygen atom remains in the solid. However, over  $3424 \text{ cm}^{-1}$  broad bands were also suggested to be an overtone of C=O bands which accompany carbonyl or a ketone functional group at  $1698 \text{ cm}^{-1}$ [34]. But at a higher temperature, the bands in this region disappeared showing that it is due to the OH functional group instead of overtone. The  $\text{CH}_3$  stretching absorption has a very weak band at around  $2922 \text{ cm}^{-1}$ . A weak absorption band near a

wavenumber of  $2200 \text{ cm}^{-1}$  is simply due to the absorption of the diamond crystal during measurements. A wide band with two maximum peaks can be noticed between  $1700 \text{ cm}^{-1}$  -  $1500 \text{ cm}^{-1}$  and shows the presence of C = O in a ketone or carboxyl functional groups. Absorption bands below  $1600 \text{ cm}^{-1}$  to  $400 \text{ cm}^{-1}$  contains vibration of mixed origin and termed as a finger print of the molecule; contains many overtone and combination bands that are distinct for individual compounds. In the infrared spectrum of certain substances, there are weak but characteristic bands that are known to be due to overtone or combination bands. So, the weak peak band near  $2927 \text{ cm}^{-1}$  is probably of the overtone of the peak near  $1463 \text{ cm}^{-1}$ , which is the asymmetric bending of  $\text{CH}_3$ . As indicated in the wave number range of  $3600 \text{ cm}^{-1}$  -  $3200 \text{ cm}^{-1}$  (Figure 3) a broad band caused by the presence of hydroxyl functional group is highly observed at a lower temperature. Moreover, the double peaks near  $1745$  -  $1545 \text{ cm}^{-1}$  is found to be more intense and become equal as the temperature of HTC reaction is increased.

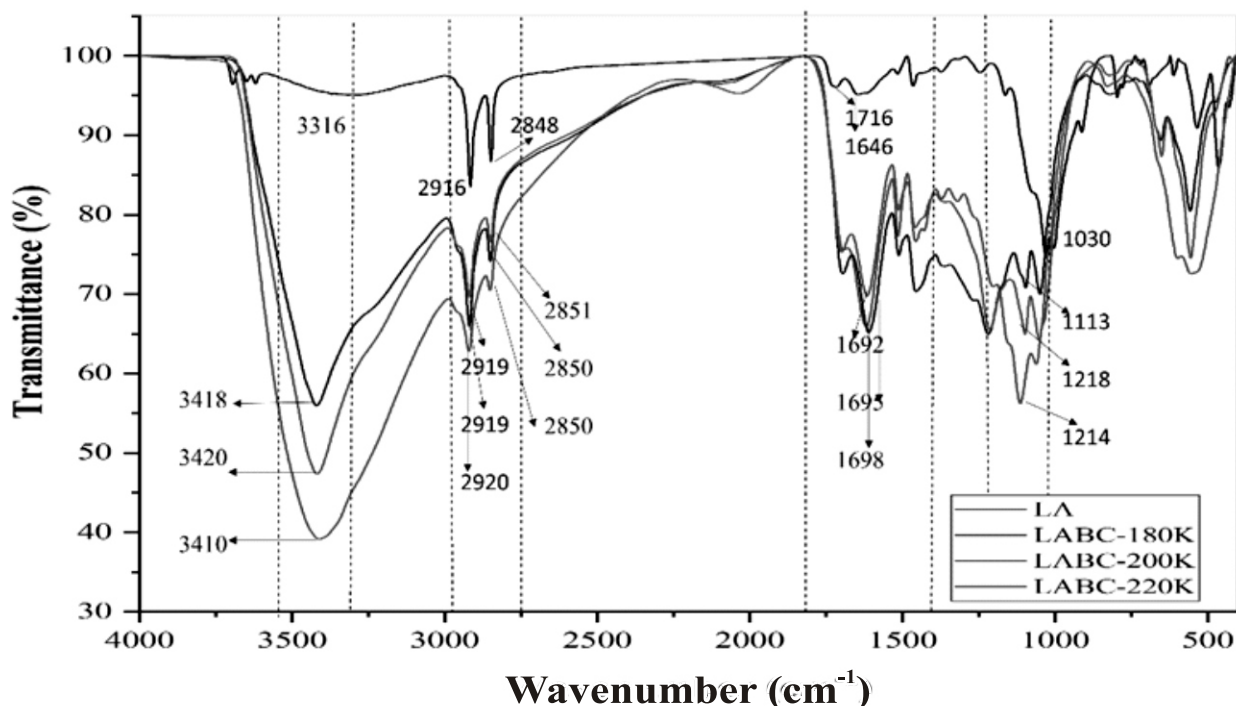
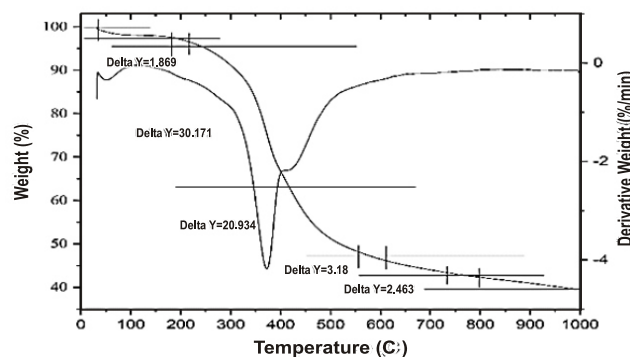


Figure 4: FTIR spectrum of raw biomass lepironia articulata along with LAHCs prepared at different temperatures

### 3.6 Thermogravimetric Analysis (TGA):

To further investigate the rate of mass loss and the stability of the hydrochar produced at 220 °C, the TGA method was employed. The temperature ranged from 30 to 1000 °C with a rate of 10 °C/min. To demonstrate the decomposition behavior of lignocellulosic biomass four sections were taken into account: (a) evaporation of moisture and devolatilization phase which occurred at temperatures under 120 °C; (b) degradation and combustion of hemicellulose, taking place at 180–250 °C; (c) breakdown of cellulose and lignin at 250–420 °C; (d) char combustion and degradation of lignin above 420 °C. The variation in the mass loss of hydrochar with respect to temperature is shown in Figure 4. A minor mass loss (about 1.869%) was observed for temperatures from 50–100 °C, which validate the removal of volatile matter and moisture content. The maximum decomposition rate was observed at temperatures from 250–450 °C. In this range, the decomposition of cellulose, hemicellulose, and lignin contents begin and sustained with an increase in temperature [15]. In connection of the statement above lignin decomposes at the temperature above 220°C, hemicelluloses decomposes at the temperature range of 180°C and 200°C and cellulose decomposes at temperature ranges above 210°C. The 50% mass of hydrochar lost was observed in this range. In continuation, 3.18% and 2.463 % mass loss was detected at temperatures ranging from 450–750 °C, which signifies the elimination of all volatile matters present in hydrochar. The almost flat temperature profile was observed between 750–1000 °C, confirming that the remaining mass left is residue after the removal of all volatiles. The TGA results confirm the stability of hydrochar to remain in the soil if used for carbon sequestration purpose as they will be more unaffected to bacterial oxidation [35].



**Figure 5:** TG and DTG curves of CR and hydrochar by HTC at 220 °C and 2 h reaction duration and biomass to water ratio of 1:10

### 3.7 Iodine value:

Iodine number is generally used as a sign of adsorption ability of a specific material. It is used to express porosity, adsorption capacity, and surface area of the activated carbon[36]. A standard test method to obtain an iodine number of hydrochars was adopted from [37]. The results to demonstrate the iodine adsorption capacity of hydrochar is shown in Figure 5. The HTC process confirmed to develop porosity of dried LA. Iodine number of hydrochars increased with increase in HTC temperature. It indicates to develop some more functional groups as soon as the volatile matters disappeared with an increase in temperature. A high iodine number of about  $220 \pm 12$  mg/g was found at 1 h for sample LAHC-240-2. Regardless of the iodine number, the tendency of hydrochars was also proved to have good adsorption capacity during the ion exchange process with other organic and inorganic contaminants present in wastewater. A study conducted by June *et al* (2015)[20] in which he confirmed the negative surface charges on hydrochars by getting the results of moderately negative zeta potential for all of the hydrochars. Thus, this finding validates the suitability of hydrochars as biosorbents of positively charged ions, such as heavy metals. Besides the developed surface functional groups the HTC temperature used here was not enough to develop high porous structure due to the reason could be the volatile

matter and tar present in the pores may block the reacting agent to get diffused into the biomass structure. Meanwhile, the longer HTC holding time may have some adverse effect on the morphological structure of the char products, i.e. the destruction of small pores may lead to diffusion and end up with minimized porosity at the end[39][41].

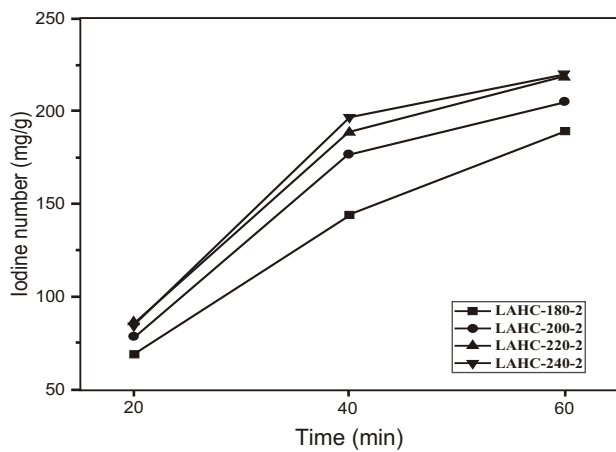


**Figure 6:** Iodine number of LAHCs against the time for adsorption

#### 4. Conclusions:

Converting biomass into valuable products through the hydrothermal carbonization process was successfully performed at different carbonization temperatures to get the maximum yield in terms of energy and char products. The highest hydrochar yield obtained was 68.8% at 180 °C which further decreased to 55.2% at 240 °C. The highest HHV value of 25.10 MJ/kg obtained at 240 °C makes it feasible for energy production. Furthermore, the optimum iodine value of 220 mg/g for sample LAHC-240-2 suggest the potential of the hydrochar as an adsorbent for the removal of organic and inorganic contaminants in wastewater, particularly heavy metals. Besides its application in wastewater treatment, LAHC can be used as an adsorbent for air and gas purification processes. The potential of hydrochar through TGA results suggest its stability in the soil if used for carbon sequestration purposes as they will be more resistant to microbial oxidation. The liquid fractions obtained have a

potential application which could be identified after analyzing and separation process as future work.

#### Acknowledgment:

This research was supported by the Higher Education Research Promotion and Thailand's Education Hub for Southern Region of ASEAN countries (TEH-AC 054/2016) Project Office of the Higher Education Commission and graduate school Prince of Songkla University.

#### References:

1. J. A. Libra, "Hydrothermal carbonization of biomass residuals: A comparative review of the chemistry, processes and applications of wet and dry pyrolysis," *Biofuels*, vol. 2, no. 1, pp. 71106, 2011.
2. N. Eibisch, "Properties and Degradability of Hydrothermal Carbonization Products," *J. Environ. Qual.*, vol. 42, no. 5, p. 1565, 2013.
3. S. Meyer, B. Glaser, and P. Quicker, "Technical, economical, and climate-related aspects of biochar production technologies: A literature review," *Environ. Sci. Technol.*, vol. 45, no. 22, pp. 94739483, 2011.
4. S. Kang, X. Li, J. Fan, and J. Chang, "Characterization of hydrochars produced by hydrothermal carbonization of lignin, cellulose, d-xylose, and wood meal," *Ind. Eng. Chem. Res.*, vol. 51, no. 26, pp. 90239031, 2012.
5. S. K. Hoekman, A. Broch, L. Felix, and W. Farthing, "Hydrothermal carbonization (HTC) of loblolly pine using a continuous, reactive twin-screw extruder," *Energy Convers. Manag.*, vol. 134, pp. 247259, 2017.
6. T. Wang, Y. Zhai, Y. Zhu, C. Li, and G. Zeng, "A review of the hydrothermal carbonization of biomass waste for hydrochar formation: Process conditions, fundamentals, and physicochemical properties," *Renew. Sustain. Energy Rev.*, vol. 90, no. March, pp. 223247, 2018.
7. D. Kalderis, M. S. Kotti, A. Méndez, and G. Gascó, "Characterization of hydrochars produced by hydrothermal carbonization of

rice husk," *Solid Earth*, vol. 5, no. 1, pp. 477483, 2014.

8. Y. Gao, H. Chen, J. Wang, T. Shi, H.-P. Yang, and X.-H. Wang, "Characterization of products from hydrothermal liquefaction and carbonation of biomass model compounds and real biomass," *J. Fuel Chem. Technol.*, vol. 39, no. 12, pp. 893900, 2011.

9. E. Danso-Boateng, G. Shama, A. D. Wheatley, S. J. Martin, and R. G. Holdich, "Hydrothermal carbonisation of sewage sludge: Effect of process conditions on product characteristics and methane production," *Bioresour. Technol.*, vol. 177, pp. 318327, 2015.

10. S. Kannan, Y. Gariepy, and G. S. V. Raghavan, "Optimization and Characterization of Hydrochar Derived from Shrimp Waste," *Energy and Fuels*, vol. 31, no. 4, pp. 40684077, 2017.

11. J. Cai, B. Li, C. Chen, J. Wang, M. Zhao, and K. Zhang, "Hydrothermal carbonization of tobacco stalk for fuel application," *Bioresour. Technol.*, vol. 220, pp. 305311, 2016.

12. M. Coronella, C.J.; Lynam, J.G.; Reza, M.T.; Uddin, Hydrothermal carbonization of lignocellulosic biomass. 2014.

13. Q. Zhu, "Coal sampling and analysis standards standards," no. April 2014.

14. F. Feng, W. Y. Liu, Y. S. Chen, Q. L. Guo, and Q. D. You, "Study on derivatives of gambogic acid," *J. China Pharm. Univ.*, vol. 36, no. 4, pp. 302305, 2005.

15. K. U. Anyikude, "Analysis of Pollutants in Biochars and Hydrochars Produced by Pyrolysis and Hydrothermal Carbonization of Waste Biomass," 2016.

16. M. T. Reza, E. Rottler, L. Herklotz, and B. Wirth, "Hydrothermal carbonization (HTC) of wheat straw: Influence of feedwater pH prepared by acetic acid and potassium hydroxide," *Bioresour. Technol.*, vol. 182, pp. 336344, 2015.

17. S. A. Channiwala and P. P. Parikh, "A unified correlation for estimating HHV of solid, liquid and gaseous fuels," *Fuel*, vol. 81, no. 8, pp. 10511063, 2002.

18. A. R. Zimmerman, "A biotic and {Microbial}\{Oxidation\} of {Laboratory}\-{Produced}\{Black\}\{Carbon\}\{Biochar\}\," *Environ. Sci. Technol.*, vol. 44, no. 4, pp. 12951301, 2010.

19. S. Kang, X. Li, J. Fan, and J. Chang, "Characterization of Hydrochars Produced by Hydrothermal Carbonization of Lignin , Cellulose , D-Xylose , and ...," no. June 2012, 2015.

20. J. Fang, B. Gao, J. Chen, and A. R. Zimmerman, "Hydrochars derived from plant biomass under various conditions: Characterization and potential applications and impacts," *Chem. Eng. J.*, vol. 267, pp. 253259, 2015.

21. F. Hu, S. Jung, and A. Ragauskas, "Bioresource Technology Pseudo-lignin formation and its impact on enzymatic hydrolysis," *Bioresour. Technol.*, vol. 117, pp. 712, 2012.

22. K. Tekin, M. K. Akalin, and S. Karagöz, "The effects of water tolerant Lewis acids on the hydrothermal liquefaction of lignocellulosic biomass," *J. Energy Inst.*, vol. 89, no. 4, pp. 627635, 2016.

23. R. Abdullah, K. Ueda, and S. Saka, "Hydrothermal decomposition of various crystalline celluloses as treated by semi-flow hot-compressed water," *J. Wood Sci.*, vol. 60, no. 4, pp. 278286, 2014.

24. K. Nakason, B. Panyapinyopol, V. Kanokkantapong, N. Viriya-empikul, W. Kraithong, and P. Pavasant, "Characteristics of hydrochar and liquid fraction from hydrothermal carbonization of cassava rhizome," *J. Energy Inst.*, vol. 91, no. 2, pp. 184193, 2018.

25. Y. Zhai, "Production of fuel pellets via hydrothermal carbonization of food waste

using molasses as a binder," *Waste Manag.*, vol. 77, pp. 185194, 2018.

26. M. T. Reza, J. G. Lynam, M. H. Uddin, and C. J. Coronella, "Hydrothermal carbonization: Fate of inorganics," *Biomass and Bioenergy*, vol. 49, pp. 8694, 2013.

27. X. Lu, P. J. Pellechia, J. R. V Flora, and N. D. Berge, "Influence of reaction time and temperature on product formation and characteristics associated with the hydrothermal carbonization of cellulose," *Bioresour. Technol.*, vol. 138, pp. 180190, 2013.

28. C. Falco, N. Baccile, and M. M. Titirici, "Morphological and structural differences between glucose, cellulose and lignocellulosic biomass derived hydrothermal carbons," *Green Chem.*, vol. 13, no. 11, pp. 32733281, 2011.

29. M. T. Reza, "Hydrothermal Carbonization of Biomass for Energy and Crop Production," *Appl. Bioenergy*, vol. 1, no. 1, pp. 1129, 2014.

30. W. Wagner, "Wagner equation," *Cryogenics (Guildf.)*, vol. 13, no. 8, pp. 470482, 1973.

31. S. Nizamuddin, N. S. Jaya Kumar, J. N. Sahu, P. Ganesan, N. M. Mubarak, and S. A. Mazari, "Synthesis and characterization of hydrochar produced by hydrothermal carbonization of oil palm shell," *Can. J. Chem. Eng.*, vol. 93, no. 11, pp. 19161921, 2015.

32. P. Stellacci, L. Liberti, M. Notarnicola, and P. L. Bishop, "Valorization of coal fly ash by mechano-chemical activation Part I . Enhancing adsorption capacity," vol. 149, pp. 1118, 2009.

33. F. Fan, Z. Zheng, Y. Liu, Y. Huang, and Z. Shi, "Preparation and characterisation of optimised hydrochar from hydrothermal carbonisation of macadamia shells," *BioResources*, vol. 13, no. 1, pp. 967980, 2018.

34. Asadullah, L. Kaewsichan, and K. Tohdee, "Prospective Sorption Evaluation of Hydrothermally Carbonized *Lepironia articulata* (Grey sedge) for the Removal of Ni (II) from Aqueous Solution," *Chiang Mai J. Sci.*, vol. 45, no. 5, pp. 22202231, 2018.

35. O. R. Harvey, L. Kuo, A. R. Zimmerman, P. Loucheuarn, J. E. Amonette, and B. E. Herbert, "An Index-Based Approach to Assessing Recalcitrance and Soil Carbon Sequestration Potential of Engineered Black Carbons (Biochars)," 2012.

36. H. Mao, D. Zhou, Z. Hashisho, S. Wang, H. Chen, and H. Wang, "Preparation of pinewood- and wheat straw-based activated carbon via a microwave-assisted potassium hydroxide treatment and an analysis of the effects of the microwave activation conditions," *BioResources*, vol. 10, no. 1, pp. 809821, 2015.

37. A. Carbon, "Standard Test Method for Determination of Iodine Number of Activated Carbon 1," vol. 94, no. Reapproved, pp. 15, 2006.

38. P. Saetea and N. Tippayawong, "Recovery of Value-Added Products from Hydrothermal Carbonization of Sewage Sludge," *ISRN Chem. Eng.*, vol. 2013, pp. 16, 2013.

39. Asadullah, L. Kaewsichan, and K. Tohdee, "Adsorption of hexavalent chromium onto alkali-modified biochar derived from *Lepironia articulata*: A kinetic, equilibrium, and thermodynamic study," *Water Environ. Res.*, pp. 114, 2019.

40. K. Tohdee, L. Kaewsichan, and Asadullah, "Enhancement of adsorption efficiency of heavy metal Cu(II) and Zn(II) onto cationic surfactant modified bentonite," *J. Environ. Chem. Eng.*, vol. 6, no. 2, pp. 28212828, 2018.

41. K. Asadullah; Kaewsichan, Lupong; Tohdee, "Potential of BCDMACl modified bentonite in simultaneous adsorption of heavy metal Ni (II) and humic acid," *J. Environ. Chem. Eng.*, vol. 6, no. 4, pp. 56165624, 2018.